



# Forced in-plane vibration of a thick ring on a unilateral elastic foundation



Chunjian Wang<sup>a,\*</sup>, Beshah Ayalew<sup>a</sup>, Timothy Rhyne<sup>b</sup>, Steve Cron<sup>b</sup>,  
Benoit Dailliez<sup>c</sup>

<sup>a</sup> Clemson University International Center for Automotive Research, No. 4 Research Dr., Greenville, SC 29607, USA

<sup>b</sup> Michelin America Research Corporation, 515 Michelin Rd., Greenville, SC 29605, USA

<sup>c</sup> Centre de Technologie Europe, Michelin Corporation Clermont Ferrand, France

## ARTICLE INFO

### Article history:

Received 26 June 2015

Received in revised form

9 June 2016

Accepted 10 June 2016

Handling Editor: H. Ouyang

Available online 29 June 2016

### Keywords:

Ring on elastic foundation

Unilateral elastic foundation

Timoshenko beam

In-plane dynamics

Iterative compensation method

## ABSTRACT

Most existing studies of a deformable ring on elastic foundation rely on the assumption of a linear foundation. These assumptions are insufficient in cases where the foundation may have a unilateral stiffness that vanishes in compression or tension such as in non-pneumatic tires and bushing bearings. This paper analyzes the in-plane dynamics of such a thick ring on a unilateral elastic foundation, specifically, on a two-parameter unilateral elastic foundation, where the stiffness of the foundation is treated as linear in the circumferential direction but unilateral (i.e. collapsible or tensionless) in the radial direction. The thick ring is modeled as an orthotropic and extensible circular Timoshenko beam. An arbitrarily distributed time-varying in-plane force is considered as the excitation. The Equations of Motion are explicitly derived and a solution method is proposed that uses an implicit Newmark scheme for the time domain solution and an iterative compensation approach to determine the unilateral zone of the foundation at each time step. The dynamic axle force transmission is also analyzed. Illustrative forced vibration responses obtained from the proposed model and solution method are compared with those obtained from a finite element model.

© 2016 Elsevier Ltd. All rights reserved.

## 1. Introduction

This paper deals with the analysis of the in-plane vibration of non-pneumatic tires [1] and other similar structures using a deformable ring on elastic foundation (REF) model, where the foundation may have a non-linear or unilateral stiffness [2,3]. The in-plane vibration of a REF [4,5] has been intensively studied due to its broad and important applications such as in tires [6–8], wheels and gears [9,10]. Most of the existing studies on REFs assume a distributed elastic foundation, whose stiffness is uniformly constant around the ring. These REF models with linear foundation assumptions can be solved analytically [5,11]. The ring resting on this linear elastic foundation has been treated using different beam models and theories. The simplest model proposed for the ring is a tensioned string that has direct tensile strain but no bending stiffness [12]. More practically, a thin ring is modeled using Euler–Bernoulli beam theory, where both the tensile and the bending stiffness are taken into account by assuming that plane cross-sections remain plane and are always normal to the neutral axis of the

*Abbreviations:* REF, ring on elastic foundation; EOMs, Equations of Motion; FEA, Finite Element Analysis

\* Corresponding author.

E-mail address: [chunjw@g.clemson.edu](mailto:chunjw@g.clemson.edu) (C. Wang).

<http://dx.doi.org/10.1016/j.jsv.2016.06.010>

0022-460X/© 2016 Elsevier Ltd. All rights reserved.

Nomenclature			
$R$	radius of ring centroid	$\sigma_{rr}, \sigma_{\theta\theta}, \tau_{r\theta}$	radial, circumferential and shear stress
$h$	thickness of ring in radial direction	$\nu$	Poisson's ratio
$b$	model width in perpendicular direction of ring plane	$U_1, U_2, T, W$	strain energy of ring, strain energy of foundation, kinetic energy of ring and work done by external force
$K_r, K_\theta$	radial and circumferential stiffness per radian of foundation	$q_r, q_\theta$	distributed external force per unit area
$E_r, E_\theta, G$	radial, circumferential and shear modulus of the ring	$F_r, F_\theta$	distributed external force per radian
$A, I$	area and area moment of inertial of ring cross-section	$Q, H$	Fourier coefficients of external force and compensation force
$C_{Er}, C_{E\theta}$	foundation viscous damping per radian in radial and circumferential direction	$a, b, c, p$	time coefficients for radial, circumferential displacement, cross-section rotation and external force
$\rho$	mass density of ring	<b>M, C, K</b>	mass, damping and stiffness matrices in Equation of Motions
$u_r, u_\theta$	radial and circumferential displacement	<b>A(t), V(t), X(t), Γ(t)</b>	acceleration, velocity, displacement and forcing vectors in Equation of Motions
$\phi$	rotation angle of ring cross-section	$\alpha, \beta$	weight coefficients in Newmark method
$r, \theta$	radial and circumferential coordinate	$\sigma$	distribution factor of Gaussian function
$t$	time	$k_r, k_\theta$	non-vanished spring element stiffness in FEA model
$n, N$	mode number and cut-off mode number		
$\epsilon_{rr}, \epsilon_{\theta\theta}, \gamma_{r\theta}$	radial, circumferential and shear strain		

ring after deformation [8,11]. Thick rings are often modeled using Timoshenko beam theory, which takes the shear deformation into account by assuming the normal of a plane cross-section is subjected to rotation in addition to the bending effects [13]. The effect of the extensibility of the ring has also been addressed by combining both thin and thick ring models with linear and uniform elastic foundations [14,4].

Allaei et al. [15], Wu and Parker [10] extended the studies to linear but non-uniform elastic foundations. Allaei et al. [15] studied the natural frequencies and mode shapes of rings supported by a number of radial spring elements attached at arbitrary locations. Wu and Parker [10] studied the free vibration of rings on a general elastic foundation, whose stiffness distribution can be different circumferentially, and gave the closed-form expression for natural frequencies and vibration modes. In this case, however, the circumferential distribution of the stiffness is fixed and known. The application of this non-uniform elastic foundation includes tires with non-uniformity and planetary gears where tooth meshes for the ring and the planets are not equally spaced.

The structure of the non-pneumatic tire invented by co-authors [1] consists of a deformable shear ring supported by collapsible spokes which buckle and lose stiffness when compressed [16]. The stiffness given by this kind of unilateral foundation typically vanishes locally in the compressed region. This unilateral REF model is also applicable to the bushing bearings, whose external sleeve can lose contact with the internal sleeve which can then be modeled as a ring on tensionless foundation. This deformation-dependent stiffness makes the dynamics of the REF model nonlinear and thus more difficult to solve. This nonlinear dynamic model can be solved via numerical methods such as Finite Element Analysis (FEA), but a parametric REF model that does not rely on discretization and mesh generation is more desirable since it can facilitate rapid design space exploration, and offer broadly useful physical insights into the major effects. However, the existing body of literature on analysis of parametric REF models with unilateral foundations is rather limited. Celep [17] studied the forced response of a thin and inextensible circular ring on tensionless two-parameter foundation under a time varying in-plane load. Direct numerical integration was used to solve the nonlinear differential equations. The circumferential displacement of the ring was obtained from the inextensible ring assumption. This approach cannot be adopted for a more general extensible Timoshenko ring. Gasmi et al. [2] studied a Timoshenko ring resting on a collapsible foundation for the analysis of non-pneumatic tires, but their work was only limited to the static problem and could not be straightforwardly extended to the dynamic case.

The present paper deals with the in-plane vibration of a deformable thick ring resting on unilateral foundation. In our companion paper [3], which focused on the static deformation of a thick ring on unilateral foundation, we proposed an iterative compensation scheme to analyze the unilateral foundation problem. The approach was built from the analytical solution of the linear foundation case by first computing the excessive force that would not be there with a unilateral foundation. Then, a compensation force is applied to the linear foundation model to counter-act this excessive force thereby setting up a simple algebraic iteration scheme to solve for the final deformation for the unilateral foundation case. In this paper, the iterative compensation approach is extended to solve the dynamic problem where the forced vibration of a thick ring on a unilateral elastic foundation is investigated. The ring is modeled as an orthotropic circular Timoshenko beam and the foundation is assumed to be a two-parameter elastic foundation, which has both radial and circumferential stiffness but the one in the radial direction is unilateral. Linear viscous damping is incorporated into the Equations of Motions (EOMs)

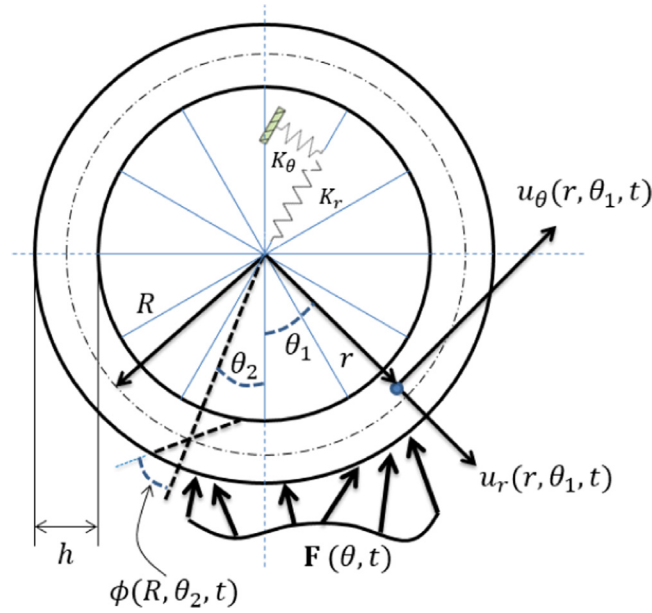


Fig. 1. Timoshenko ring on two-parameter elastic foundation.

using Rayleigh’s dissipation functions via the extended Hamilton’s principle [18]. We adopted the implicit discrete integration scheme via the Newmark method to solve the time response for the unilateral foundation problem. At every time step, the iterative compensation approach mentioned above is implemented to obtain the spatial response. This iterative compensation scheme solves the unilateral foundation problem via simple algebraic iterations. Thereby, it avoids time-consuming matrix inversions needed in conventional implicit integration methods.

The rest of the paper is organized as follows. Section 2 re-states the problem and develops the Equations of Motion (EOMs). Section 3 gives the solution for both the linear and unilateral foundation cases and analyzes the axle force transmission. In Section 4, application examples are given considering responses to pulse and chirp concentrated force cases to illustrate the effectiveness of the proposed method. Results are validated via comparisons with FEA results. Section 5 concludes the paper and discusses the future work.

2. Statement of problem and Equation of Motions

Fig. 1 shows the schematic of the REF model. The ring with thickness *h* is assumed to have a radius *R* at its centroid. The width perpendicular to the plane of the ring is *b*. The uniformly distributed radial and circumferential stiffnesses are assumed to be *K<sub>r</sub>* and *K<sub>θ</sub>*, respectively. These have units of stiffness per radian. For a linear elastic foundation, the distributed radial stiffness *K<sub>r</sub>* is constant and invariant around the ring. Equations of Motion (EOMs) are first obtained based on this linear foundation assumption. However, for the unilateral elastic foundation, the radial stiffness vanishes in locations where the elastic foundation is tensioned or compressed. This unilateral foundation problem will be addressed in the solution procedure presented in Section 3. A local polar coordinate system with the origin located at the ring center is adopted. The center of the ring is fixed.

At time *t*, the radial and circumferential displacements at circumferential location *θ* of the ring centroid are assumed to be *u<sub>r</sub>(R, θ, t)* and *u<sub>θ</sub>(R, θ, t)*, respectively. Following Timoshenko beam assumption [19], the thickness of the ring is invariant, i.e., the radial displacement of an arbitrary point is the same for same circumferential coordinate *θ*, regardless of the radius. This assumption implies no radial strain through the thickness of the ring. The cross-section of the ring is assumed to have a rotation *φ(R, θ, t)* and keeps its plane after deformation. Then, the radial and circumferential displacements at an arbitrary point on the ring with radius *r* and circumferential coordinate *θ*, *u<sub>r</sub>(r, θ, t)* and *u<sub>θ</sub>(r, θ, t)*, can be represented by:

$$\begin{aligned} u_r(r, \theta, t) &= u_r(R, \theta, t) \\ u_\theta(r, \theta, t) &= u_\theta(R, \theta, t) + (r - R)\phi(R, \theta, t) \end{aligned} \tag{1}$$

The strain–displacement relationships in polar coordinates are [20]:

$$\begin{aligned} \epsilon_{rr}(r, \theta, t) &= \frac{\partial}{\partial r} u_r(r, \theta, t) = 0 \\ \epsilon_{\theta\theta}(r, \theta, t) &= \frac{1}{r} \frac{\partial}{\partial \theta} u_\theta(r, \theta, t) + \frac{1}{r} u_r(r, \theta, t) \end{aligned}$$

$$\gamma_{r\theta}(r, \theta, t) = \frac{1}{r} \frac{\partial}{\partial \theta} u_r(r, \theta, t) + \frac{\partial}{\partial r} u_\theta(r, \theta, t) - \frac{1}{r} u_\theta(r, \theta, t) \tag{2}$$

where  $\epsilon_{rr}(r, \theta, t)$ ,  $\epsilon_{\theta\theta}(r, \theta, t)$ ,  $\gamma_{r\theta}(r, \theta, t)$  are the radial, circumferential and shear strains, respectively.

The ring is assumed to be orthotropic and homogeneous. The stress–strain relationships are [20]:

$$\begin{aligned} \sigma_{rr}(r, \theta, t) &= \frac{E_r (\nu_{\theta r} \epsilon_{\theta\theta}(r, \theta, t) + \epsilon_{rr}(r, \theta, t))}{-\nu_{r\theta} \nu_{\theta r} + 1} \\ \sigma_{\theta\theta}(r, \theta, t) &= \frac{E_\theta (\nu_{r\theta} \epsilon_{rr}(r, \theta, t) + \epsilon_{\theta\theta}(r, \theta, t))}{-\nu_{r\theta} \nu_{\theta r} + 1} \\ \tau_{r\theta}(r, \theta, t) &= G \gamma_{r\theta}(r, \theta, t) \end{aligned} \tag{3}$$

where  $\sigma_{rr}(r, \theta, t)$ ,  $\sigma_{\theta\theta}(r, \theta, t)$  and  $\tau_{r\theta}(r, \theta, t)$  are radial, circumferential and shear stresses, respectively.  $E_r$ ,  $E_\theta$  and  $G$  are elastic modulus in the radial and circumferential directions and the shear modulus, respectively.  $\nu$  represents the Poisson’s ratio, and the subscript  $ij$  indicates the effect is from direction  $i$  to direction  $j$ .

The strain energy change in the ring from time  $t_0$  to  $t_1$  is obtained from:

$$U_1 = \frac{b}{2} \int_{t_0}^{t_1} \int_{-\pi}^{\pi} \int_{R-\frac{h}{2}}^{R+\frac{h}{2}} (\sigma_{rr}\epsilon_{rr} + \sigma_{\theta\theta}\epsilon_{\theta\theta} + \tau_{r\theta}\gamma_{r\theta}) r \, dr \, d\theta \, dt \tag{4}$$

For a linear foundation, the strain energy change in the elastic foundation from time  $t_0$  to  $t_1$  is obtained from:

$$U_2 = \frac{1}{2} \int_{t_0}^{t_1} \int_{-\pi}^{\pi} \left( K_r \left( u_r \left( R - \frac{h}{2}, \theta, t \right) \right)^2 + K_\theta \left( u_\theta \left( R - \frac{h}{2}, \theta, t \right) \right)^2 \right) d\theta \, dt \tag{5}$$

Note here that the radial and circumferential displacements for the internal edge of the ring  $u_r(R-\frac{h}{2}, \theta, t)$  and  $u_\theta(R-\frac{h}{2}, \theta, t)$  couple the ring and the elastic foundation.

The kinetic energy change of the ring within time interval  $[t_0, t_1]$  is:

$$T = \frac{\rho b}{2} \int_{t_0}^{t_1} \int_{-\pi}^{\pi} \int_{R-\frac{h}{2}}^{R+\frac{h}{2}} \left[ \left( \frac{\partial}{\partial t} u_r(r, \theta, t) \right)^2 + \left( \frac{\partial}{\partial t} u_\theta(r, \theta, t) \right)^2 \right] r \, dr \, d\theta \, dt \tag{6}$$

where  $\rho$  is the mass density of the ring.

The work done by the applied forces is obtained by:

$$W = b \int_{t_0}^{t_1} \int_{-\pi}^{\pi} \left( q_r u_r \left( R + \frac{h}{2}, \theta, t \right) + q_\theta u_\theta \left( R + \frac{h}{2}, \theta, t \right) \right) \left( R + \frac{h}{2} \right) d\theta \, dt \tag{7}$$

where  $q_r = q_r(R+\frac{h}{2}, \theta, t)$  and  $q_\theta = q_\theta(R+\frac{h}{2}, \theta, t)$  are time variant distributed forces applied to the external edge of the ring (at the radial location  $R+\frac{h}{2}$ ) in radial and circumferential directions, respectively. The units of  $q_r$  and  $q_\theta$  are in Pa.

Invoking Hamilton’s principle [20]:

$$\delta(U_1 + U_2 - T) = \delta W \tag{8}$$

the EOM for the conservative system can be obtained via Eq. (8).

We then introduce viscous damping using the concept of the Rayleigh’s dissipation function [21]:

$$\begin{aligned} \zeta_{Er} &= \frac{1}{2} C_{Er} \left( \frac{\partial}{\partial t} u_r \left( R - \frac{h}{2}, \theta, t \right) \right)^2 \\ \zeta_{E\theta} &= \frac{1}{2} C_{E\theta} \left( \frac{\partial}{\partial t} u_\theta \left( R - \frac{h}{2}, \theta, t \right) \right)^2 \end{aligned} \tag{9}$$

where  $\zeta_{Er}$  and  $\zeta_{E\theta}$  are Rayleigh’s dissipation functions for the radial and circumferential direction of the elastic foundation, respectively;  $C_{Er}$  and  $C_{E\theta}$  represent the viscous damping densities in the radial and circumferential directions for the elastic foundation, respectively. The unit of  $C_{Er}$  and  $C_{E\theta}$  is  $\text{Nsradian}^{-1}\text{m}^{-1}$ . Applying the extended Hamilton’s principle [18], the EOM for the non-conservative system, i.e. system with damping, can be obtained from:

$$\delta(U_1 + U_2 - T) + R_E = \delta W \tag{10}$$

where  $R_E$  is defined as:

$$R_E = \int_{t_0}^{t_1} \int_{-\pi}^{\pi} \left[ \left( \frac{\partial \zeta_{Er}}{\partial \left( \frac{\partial}{\partial t} u_r \left( R - \frac{h}{2}, \theta, t \right) \right)} \right) \delta u_r \left( R - \frac{h}{2}, \theta, t \right) + \left( \frac{\partial \zeta_{E\theta}}{\partial \left( \frac{\partial}{\partial t} u_\theta \left( R - \frac{h}{2}, \theta, t \right) \right)} \right) \delta u_\theta \left( R - \frac{h}{2}, \theta, t \right) \right] d\theta \, dt \tag{11}$$

After substitution of Eq. (1) to Eq. (7) and Eq. (11) into Eq. (10) and some manipulations according to the Euler–Lagrange equation, the final EOMs are found to be as follows:

$$-\frac{GA}{Rb} \frac{\partial^2}{\partial \theta^2} u_r + \left( \frac{EA_\theta}{(1-\nu_{r\theta} \nu_{\theta r})Rb} + \frac{K_r}{b} \right) u_r + \left( \frac{EA_\theta}{(1-\nu_{r\theta} \nu_{\theta r})Rb} + \frac{GA}{Rb} \right) \frac{\partial}{\partial \theta} u_\theta - \frac{GA}{b} \frac{\partial}{\partial \theta} \phi$$

$$\begin{aligned}
 & + \rho R h \frac{\partial^2}{\partial t^2} u_r + \frac{C_{Er}}{b} \frac{\partial}{\partial t} u_r = q_r \left( R + \frac{h}{2} \right) \\
 & \left( -\frac{EA_\theta}{(1-\nu_{r\theta}\nu_{\theta r})Rb} - \frac{GA}{Rb} \right) \frac{\partial}{\partial \theta} u_r - \frac{EA_\theta}{(1-\nu_{r\theta}\nu_{\theta r})Rb} \frac{\partial^2}{\partial \theta^2} u_\theta + \left( \frac{GA}{Rb} + \frac{K_\theta}{b} \right) u_\theta + \left( -\frac{GA}{b} - \frac{1}{2} \frac{K_\theta h}{b} \right) \phi \\
 & + \rho R h \frac{\partial^2}{\partial t^2} u_\theta + \frac{C_{E\theta}}{b} \frac{\partial}{\partial t} u_\theta + \frac{1}{12} \rho h^3 \frac{\partial^2}{\partial t^2} \phi - \frac{1}{2} \frac{C_{E\theta} h}{b} \frac{\partial}{\partial t} \phi = q_\theta \left( R + \frac{h}{2} \right) \\
 & \frac{GA}{b} \frac{\partial}{\partial \theta} u_r + \left( -\frac{GA}{b} - \frac{1}{2} \frac{K_\theta h}{b} \right) u_\theta - \frac{EI_\theta}{(1-\nu_{r\theta}\nu_{\theta r})Rb} \frac{\partial^2}{\partial \theta^2} \phi + \left( \frac{GAR}{b} + \frac{1}{4} \frac{K_\theta h^2}{b} \right) \phi + \frac{1}{12} \rho h^3 \frac{\partial^2}{\partial t^2} u_\theta \\
 & - \frac{1}{2} \frac{C_{E\theta} h}{b} \frac{\partial}{\partial t} u_\theta + \frac{1}{12} \rho R h^3 \frac{\partial^2}{\partial t^2} \phi + \frac{1}{4} \frac{C_{E\theta} h^2}{b} \frac{\partial}{\partial t} \phi = \frac{1}{2} q_\theta h \left( R + \frac{h}{2} \right)
 \end{aligned} \tag{12}$$

where the following short hand is adopted:

$$\begin{aligned}
 u_r &= u_r(R, \theta, t) \\
 u_\theta &= u_\theta(R, \theta, t) \\
 \phi &= \phi(R, \theta, t) \\
 q_r &= q_r \left( R + \frac{h}{2}, \theta, t \right) \\
 q_\theta &= q_\theta \left( R + \frac{h}{2}, \theta, t \right)
 \end{aligned} \tag{13}$$

and

$$\begin{aligned}
 EA_\theta &= E_\theta A \\
 GA &= G A \\
 EI_\theta &= E_\theta I
 \end{aligned} \tag{14}$$

with  $A = b h$  is the cross-sectional area of the ring and  $I = \frac{1}{12} b h^3$  is the area moment of inertia of the cross-section. The following approximations are used in the manipulations to obtain the governing equations, considering the case that  $R \gg h$ :

$$\begin{aligned}
 \int_{R-\frac{h}{2}}^{R+\frac{h}{2}} \frac{1}{r} dr &\approx \frac{1}{R} \int_{R-\frac{h}{2}}^{R+\frac{h}{2}} dr = \frac{h}{R} \\
 \int_{R-\frac{h}{2}}^{R+\frac{h}{2}} \frac{(r-R)}{r} dr &\approx \frac{1}{R} \int_{R-\frac{h}{2}}^{R+\frac{h}{2}} (r-R) dr = 0 \\
 \int_{R-\frac{h}{2}}^{R+\frac{h}{2}} \frac{(r-R)^2}{r} dr &\approx \frac{1}{R} \int_{R-\frac{h}{2}}^{R+\frac{h}{2}} (r-R)^2 dr = \frac{1}{12} \frac{h^3}{R}
 \end{aligned} \tag{15}$$

### 3. Solutions for the EOMs

While our objective is to solve the EOMs for the dynamics of the ring on a unilateral elastic foundation, we step through the solution for the linear elastic foundation case as it is a building block for the iterative approach we construct later.

#### 3.1. Solutions for linear elastic foundation

In this subsection, the EOMs Eq. (12) are solved for the linear foundation with constant stiffness around the ring. We start by writing an arbitrary time-variant force as a general one consisting of radial and circumferential components:

$$\mathbf{F}(\theta, t) = F_r(\theta, t)\mathbf{r} + F_\theta(\theta, t)\boldsymbol{\theta} \tag{16}$$

Each component can be expanded into a Fourier series on  $[-\pi, \pi]$ , with corresponding time-variant coefficients:

$$\begin{aligned}
 F_r(\theta, t) &= p_{r,c}(t) \sum_{n=-N}^N Q_{n,r,c} \cos(n\theta) + p_{r,s}(t) \sum_{n=-N}^N Q_{n,r,s} \sin(n\theta) \\
 F_\theta(\theta, t) &= p_{\theta,c}(t) \sum_{n=-N}^N Q_{n,\theta,c} \cos(n\theta) + p_{\theta,s}(t) \sum_{n=-N}^N Q_{n,\theta,s} \sin(n\theta)
 \end{aligned} \tag{17}$$

where  $N$  is the cut-off harmonic number,  $Q_{n,r,c}, Q_{n,r,s}, Q_{n,\theta,c}$  and  $Q_{n,\theta,s}$  are corresponding coefficients of the  $n^{th}$  harmonic force;  $p_{r,c}, p_{r,s}, p_{\theta,c}$  and  $p_{\theta,s}$  are corresponding time-variant coefficients. The subscript  $r$  or  $\theta$  indicates whether the coefficient is for the radial or circumferential direction, respectively; while  $c$  or  $s$  represents cosine or sine components, respectively. Then, the distributed force per unit area applied to the external edge of the ring can be written in terms of corresponding

components as:

$$\begin{aligned}
 q_r\left(R+\frac{h}{2}, \theta, t\right) &= \frac{F_r(\theta, t)}{b\left(R+\frac{h}{2}\right)} \\
 &= \sum_{n=-N}^N \frac{p_{r,c}(t)}{b\left(R+\frac{h}{2}\right)} Q_{n,r,c} \cos(n\theta) + \sum_{n=-N}^N \frac{p_{r,s}(t)}{b\left(R+\frac{h}{2}\right)} Q_{n,r,s} \sin(n\theta) \\
 &= \sum_{n=-N}^N q_{n,r,c}\left(R+\frac{h}{2}, \theta, t\right) + \sum_{n=-N}^N q_{n,r,s}\left(R+\frac{h}{2}, \theta, t\right) \\
 q_\theta\left(R+\frac{h}{2}, \theta, t\right) &= \frac{F_\theta(\theta, t)}{b\left(R+\frac{h}{2}\right)} \\
 &= \sum_{n=-N}^N \frac{p_{\theta,c}(t)}{b\left(R+\frac{h}{2}\right)} Q_{n,\theta,c} \cos(n\theta) + \sum_{n=-N}^N \frac{p_{\theta,s}(t)}{b\left(R+\frac{h}{2}\right)} Q_{n,\theta,s} \sin(n\theta) \\
 &= \sum_{n=-N}^N q_{n,\theta,c}\left(R+\frac{h}{2}, \theta, t\right) + \sum_{n=-N}^N q_{n,\theta,s}\left(R+\frac{h}{2}, \theta, t\right)
 \end{aligned} \tag{18}$$

From Eq. (18), the forcing functions on the right hand sides of EOMs Eq. (12) have been written in four components, representing the permutations of radial or circumferential directions and cosine or sine components, respectively. Then, a solution of Eq. (12) can be sought in the following corresponding form:

$$\begin{aligned}
 u_r(R, \theta, t) &= \sum_{n=-N}^N u_{r,n,r,c}(R, \theta, t) + \sum_{n=-N}^N u_{r,n,r,s}(R, \theta, t) + \sum_{n=-N}^N u_{r,n,\theta,c}(R, \theta, t) + \sum_{n=-N}^N u_{r,n,\theta,s}(R, \theta, t) \\
 u_\theta(R, \theta, t) &= \sum_{n=-N}^N u_{\theta,n,r,c}(R, \theta, t) + \sum_{n=-N}^N u_{\theta,n,r,s}(R, \theta, t) + \sum_{n=-N}^N u_{\theta,n,\theta,c}(R, \theta, t) + \sum_{n=-N}^N u_{\theta,n,\theta,s}(R, \theta, t) \\
 \phi(R, \theta, t) &= \sum_{n=-N}^N \phi_{n,r,c}(R, \theta, t) + \sum_{n=-N}^N \phi_{n,r,s}(R, \theta, t) + \sum_{n=-N}^N \phi_{n,\theta,c}(R, \theta, t) + \sum_{n=-N}^N \phi_{n,\theta,s}(R, \theta, t)
 \end{aligned} \tag{19}$$

To outline the solution procedure, for simplicity, only the solutions for the cosine component in the radial direction of  $n^{\text{th}}$  harmonic (i.e.,  $u_{r,n,r,c}(R, \theta, t)$ ,  $u_{\theta,n,r,c}(R, \theta, t)$  and  $\phi_{n,r,c}(R, \theta, t)$  under force component  $q_{n,r,c}(R+\frac{h}{2}, \theta, t)$ ) are shown here. The coefficients for the other permutations can be solved for in a similar way.

Note that in Eq. (18), the forcing contribution  $q_{n,r,c}(R+\frac{h}{2}, \theta, t)$  has been written in terms of the product of a time-variant coefficient and spatial distribution term:

$$q_{n,r,c}\left(R+\frac{h}{2}, \theta, t\right) = p_{r,c}(t) \frac{1}{b\left(R+\frac{h}{2}\right)} Q_{n,r,c} \cos(n\theta) = p_{r,c}(t) q_{n,r,c}\left(R+\frac{h}{2}, \theta\right) \tag{20}$$

Similarly, the solutions under this forcing function can be written in terms of products of corresponding time-variant coefficients and spatially distributed but time-invariant terms:

$$\begin{aligned}
 u_{r,n,r,c}(R, \theta, t) &= a_{n,r,c}(t) u_{r,n,r,c}(R, \theta) \\
 u_{\theta,n,r,c}(R, \theta, t) &= b_{n,r,c}(t) u_{\theta,n,r,c}(R, \theta) \\
 \phi_{n,r,c}(R, \theta, t) &= c_{n,r,c}(t) \phi_{n,r,c}(R, \theta)
 \end{aligned} \tag{21}$$

After substitution of Eqs. (20) and (21) into EOMs Eq. (12) and collection of the time coefficients, Eq. (12) can be written in the following form:

$$\begin{aligned}
 Ca_{2,1} \left(\frac{d^2}{dt^2} a_{n,r,c}(t)\right) + Ca_{1,1} \left(\frac{d}{dt} a_{n,r,c}(t)\right) + Ca_{0,1} a_{n,r,c}(t) + Cb_{0,1} b_{n,r,c}(t) + Cc_{0,1} c_{n,r,c}(t) \\
 = Cp_1 \cdot p_{r,c}(t) \\
 Cb_{2,2} \left(\frac{d^2}{dt^2} b_{n,r,c}(t)\right) + Cc_{2,2} \left(\frac{d^2}{dt^2} c_{n,r,c}(t)\right) + Cb_{1,2} \left(\frac{d}{dt} b_{n,r,c}(t)\right) + Cc_{1,2} \left(\frac{d}{dt} c_{n,r,c}(t)\right) + Ca_{0,2} a_{n,r,c}(t) \\
 + Cb_{0,2} b_{n,r,c}(t) + Cc_{0,2} c_{n,r,c}(t) = Cp_2 \cdot p_{r,c}(t) \\
 Cb_{2,3} \left(\frac{d^2}{dt^2} b_{n,r,c}(t)\right) + Cc_{2,3} \left(\frac{d^2}{dt^2} c_{n,r,c}(t)\right) + Cb_{1,3} \left(\frac{d}{dt} b_{n,r,c}(t)\right) + Cc_{1,3} \left(\frac{d}{dt} c_{n,r,c}(t)\right) \\
 + Ca_{0,3} a_{n,r,c}(t) + Cb_{0,3} b_{n,r,c}(t) + Cc_{0,3} c_{n,r,c}(t) = Cp_3 \cdot p_{r,c}(t)
 \end{aligned} \tag{22}$$

where coefficients  $Ca$ ,  $Cb$ ,  $Cc$  and  $Cp$  contain system parameters such as those listed in Table 1 as well as spatially distributed variables  $u_{r,n,r,c}(R, \theta)$ ,  $u_{\theta,n,r,c}(R, \theta)$  and  $\phi_{n,r,c}(R, \theta)$ . Their detailed expressions are listed in Appendix A.

**Table 1**  
Values of parameters.

Parameters	Definitions	Units	Values
$R$	Centroid radius	m	0.2
$b$	Model width	m	0.06
$h$	Ring thickness	m	0.02
$K_r$	Radial stiffness per radian of foundation	Nradian <sup>-1</sup> m <sup>-1</sup>	$1 \times 10^5$
$K_\theta$	Circumferential stiffness per radian of foundation	Nradian <sup>-1</sup> m <sup>-1</sup>	$1 \times 10^4$
$E_\theta$	Extensional modulus of the ring	Pa	$1 \times 10^{10}$
$G$	Shear modulus of the ring	Pa	$4 \times 10^6$
$C_{Er}$	Viscous damping density in radial direction of foundation	Nsradian <sup>-1</sup> m <sup>-1</sup>	0/50
$C_{E\theta}$	Viscous damping density in circumferential direction of foundation	Nsradian <sup>-1</sup> m <sup>-1</sup>	0/50
$Q$	magnitude of the concentrated force	N	-1000
$N$	Cut-off mode number	NA	50
$\rho$	Mass density of ring	kgm <sup>-3</sup>	$5 \times 10^3$
$\sigma$	Distribution factor of Gaussian function	NA	0.02
$\Delta t$	Time step	s	$1 \times 10^{-4}$
$\delta_u$	Convergence threshold for displacements in iterative Compensation method	m	$1 \times 10^{-4}$

In order to solve these spatially distributed variables  $u_{r,n,r,c}(R, \theta)$ ,  $u_{\theta,n,r,c}(R, \theta)$  and  $\phi_{n,r,c}(R, \theta)$ , all the time-dependent coefficients in Eq. (22) can be set identically to 1:

$$a_{n,r,c}(t) = b_{n,r,c}(t) = c_{n,r,c}(t) \equiv 1 \tag{23}$$

These give the governing equations for the static case. Replacing the coefficients  $Ca, Cb, Cc$  and  $Cp$  by their detailed expressions, one obtains:

$$\begin{aligned} &-\frac{GA}{bR} \frac{\partial^2}{\partial \theta^2} u_{r,n,r,c} + \left( -\frac{EA_\theta}{(\nu_{\theta r} \nu_{r\theta} - 1)Rb} + \frac{K_r}{b} \right) u_{r,n,r,c} + \left( \frac{GA}{bR} - \frac{EA_\theta}{(\nu_{\theta r} \nu_{r\theta} - 1)Rb} \right) \frac{\partial}{\partial \theta} u_{\theta,n,r,c} - \frac{GA}{b} \frac{\partial}{\partial \theta} \phi_{n,r,c} = \frac{Q_{nrc} \cos(n\theta)}{b} \\ &\left( \frac{EA_\theta}{(\nu_{\theta r} \nu_{r\theta} - 1)Rb} - \frac{GA}{bR} \right) \frac{\partial}{\partial \theta} u_{r,n,r,c} + \frac{EA_\theta}{(\nu_{\theta r} \nu_{r\theta} - 1)Rb} \frac{\partial^2}{\partial \theta^2} u_{\theta,n,r,c} + \left( \frac{GA}{bR} + \frac{K_\theta}{b} \right) u_{\theta,n,r,c} - \left( \frac{GA}{b} + \frac{K_\theta h}{2b} \right) \phi_{n,r,c} = 0 \\ &\frac{GA}{b} \frac{\partial}{\partial \theta} u_{r,n,r,c} - \left( \frac{AG}{b} + \frac{K_\theta h}{2b} \right) u_{\theta,n,r,c} + \frac{EI_\theta}{(\nu_{\theta r} \nu_{r\theta} - 1)Rb} \frac{\partial^2}{\partial \theta^2} \phi_{n,r,c} + \left( \frac{GA \cdot R}{b} + \frac{h^2 K_\theta}{4b} \right) \phi_{n,r,c} = 0 \end{aligned} \tag{24}$$

The governing equations in Eq. (24) are similar to the static governing equations in our previous paper [3], which only treated the case where  $\nu_{r\theta} = \nu_{\theta r} = 0$ . The solutions for  $u_{r,n,r,c}(R, \theta)$ ,  $u_{\theta,n,r,c}(R, \theta)$  and  $\phi_{n,r,c}(R, \theta)$  can be obtained via the same solution procedure as in [3] and revised here in Appendix B.

The spatial distributions  $u_{r,n,r,c}(R, \theta)$ ,  $u_{\theta,n,r,c}(R, \theta)$  and  $\phi_{n,r,c}(R, \theta)$  are then substituted into  $Ca, Cb, Cc$  of EOMs Eq. (22), so that only time coefficients  $a_{n,r,c}(t)$ ,  $b_{n,r,c}(t)$ ,  $c_{n,r,c}(t)$  remain unknown in the EOMs. To solve these time coefficients, Eq. (22) is written in the mass-spring-damper form:

$$\mathbf{M}_{n,r,c} \mathbf{A}_{n,r,c}(t) + \mathbf{C}_{n,r,c} \mathbf{V}_{n,r,c}(t) + \mathbf{K}_{n,r,c} \mathbf{X}_{n,r,c}(t) = \mathbf{\Gamma}_{n,r,c}(t) \tag{25}$$

where the vectors are given by:

$$\mathbf{A}_{n,r,c}(t) = \begin{bmatrix} \frac{\partial^2}{\partial t^2} a_{n,r,c}(t) \\ \frac{\partial^2}{\partial t^2} b_{n,r,c}(t) \\ \frac{\partial^2}{\partial t^2} c_{n,r,c}(t) \end{bmatrix} \quad \mathbf{V}_{n,r,c}(t) = \begin{bmatrix} \frac{\partial}{\partial t} a_{n,r,c}(t) \\ \frac{\partial}{\partial t} b_{n,r,c}(t) \\ \frac{\partial}{\partial t} c_{n,r,c}(t) \end{bmatrix} \quad \mathbf{X}_{n,r,c}(t) = \begin{bmatrix} a_{n,r,c}(t) \\ b_{n,r,c}(t) \\ c_{n,r,c}(t) \end{bmatrix} \tag{26}$$

And:

$$\mathbf{\Gamma}_{n,r,c}(t) = \begin{bmatrix} \frac{Q_{n,r,c} \cos(n\theta) p_{r,c}(t)}{b} \\ 0 \\ 0 \end{bmatrix} = p_{r,c}(t) \begin{bmatrix} \frac{Q_{n,r,c} \cos(n\theta)}{b} \\ 0 \\ 0 \end{bmatrix} = p_{r,c}(t) \mathbf{\Gamma}_{n,r,c}^S \tag{27}$$

where  $\mathbf{\Gamma}_{n,r,c}^S$  is a time-invariant forcing vector.  $\mathbf{M}_{n,r,c}$ ,  $\mathbf{C}_{n,r,c}$ ,  $\mathbf{K}_{n,r,c}$  are the mass, damping, stiffness matrices, respectively. They can be obtained easily in terms of coefficients  $Ca, Cb, Cc$  following standard procedures.

A State-Space form can also be obtained via further manipulation of Eq. (25):

$$\dot{\mathbf{Y}}_{n,r,c}(t) = \mathbf{L}_{n,r,c} \mathbf{Y}_{n,r,c}(t) + \mathbf{U}_{n,r,c}(t) \tag{28}$$

where the state vector is:

$$\mathbf{Y}_{n,r,c}(t) = \left[ a_{n,r,c}(t) \quad \frac{\partial}{\partial t} a_{n,r,c}(t) \quad b_{n,r,c}(t) \quad \frac{\partial}{\partial t} b_{n,r,c}(t) \quad c_{n,r,c}(t) \quad \frac{\partial}{\partial t} c_{n,r,c}(t) \right]^T \tag{29}$$

The analytical solution for Eq. (28) exists and is given by:

$$\mathbf{Y}_{n,r,c}(t) = e^{\mathbf{L}_{n,r,c} \cdot t} \mathbf{Y}_{n,r,c}(0) + \int_0^t \mathbf{U}_{n,r,c}(\tau) e^{\mathbf{L}_{n,r,c} \cdot (t-\tau)} d\tau \quad (30)$$

where  $\mathbf{Y}_{n,r,c}(0)$  is the initial value of the state vector. Matrices  $\mathbf{L}_{n,r,c}$ ,  $\mathbf{U}_{n,r,c}(t)$  can be assembled following standard procedures so they are omitted here for brevity. The components of the solved for state vector  $\mathbf{Y}_{n,r,c}(t)$  can then be used to construct the dynamic solutions using Eq. (21).

### 3.2. Solution for ring on unilateral elastic foundation

In this subsection, the case of the (nonlinear) unilateral foundation is treated. In this case, analytical solutions of Eq. (25) are not straightforward to implement with the iterative force compensation scheme to be outlined below. Instead, the classical Newmark method [22] is adopted to implicitly solve the mass-spring-damper system given by Eq. (25). It proceeds as follows (see Eq. (26) for definitions of vectors):

$$\begin{aligned} \mathbf{V}_{n,r,c}(t+\Delta t) &= \mathbf{V}_{n,r,c}(t) + ((1-\alpha)\mathbf{A}_{n,r,c}(t+\Delta t) + \alpha\mathbf{A}_{n,r,c}(t))\Delta t \\ \mathbf{X}_{n,r,c}(t+\Delta t) &= \mathbf{X}_{n,r,c}(t) + \Delta t \mathbf{V}_{n,r,c}(t) + \left(\beta\mathbf{A}_{n,r,c}(t+\Delta t) + \left(\frac{1}{2}-\beta\right)\mathbf{A}_{n,r,c}(t)\right)\Delta t^2 \end{aligned} \quad (31)$$

where  $\Delta t$  is the time step.  $\alpha$  and  $\beta$  are weight coefficients, and the average acceleration method with  $\alpha = \frac{1}{2}$ ,  $\beta = \frac{1}{4}$  is adopted. Combining Eqs. (25) and (31), the displacement increment for every time step can be obtained by:

$$\begin{aligned} \Delta\mathbf{X}_{n,r,c}(t+\Delta t) &= \frac{1}{2} \frac{\Delta t (\mathbf{C}_{n,r,c}\alpha\Delta t^2 + 2\mathbf{C}_{n,r,c}\beta\Delta t^2 - \mathbf{C}_{n,r,c}\Delta t^2 - \mathbf{M}_{n,r,c}\Delta t)}{-\mathbf{K}_{n,r,c}\beta\Delta t^2 + \mathbf{C}_{n,r,c}\alpha\Delta t - \mathbf{C}_{n,r,c}\Delta t - \mathbf{M}_{n,r,c}} \mathbf{A}_{n,r,c}(t) \\ &+ \frac{1}{2} \frac{\Delta t (2\mathbf{C}_{n,r,c}\alpha\Delta t - 2\mathbf{C}_{n,r,c}\Delta t - 2\mathbf{M}_{n,r,c})}{-\mathbf{K}_{n,r,c}\beta\Delta t^2 + \mathbf{C}_{n,r,c}\alpha\Delta t - \mathbf{C}_{n,r,c}\Delta t - \mathbf{M}_{n,r,c}} \mathbf{V}_{n,r,c}(t) \\ &- \frac{\Delta t^2\beta}{-\mathbf{K}_{n,r,c}\beta\Delta t^2 + \mathbf{C}_{n,r,c}\alpha\Delta t - \mathbf{C}_{n,r,c}\Delta t - \mathbf{M}_{n,r,c}} \Delta\mathbf{\Gamma}_{n,r,c}(t+\Delta t) \end{aligned} \quad (32)$$

Then the obtained displacement for the current time step:

$$\mathbf{X}_{n,r,c}(t+\Delta t) = \mathbf{X}_{n,r,c}(t) + \Delta\mathbf{X}_{n,r,c}(t+\Delta t) \quad (33)$$

$\mathbf{A}_{n,r,c}(t+\Delta t)$  and  $\mathbf{V}_{n,r,c}(t+\Delta t)$  can be solved by substitution of Eq. (33) into Eq. (31). The incremental forcing vector  $\Delta\mathbf{\Gamma}_{n,r,c}(t+\Delta t)$  in (32) is given by:

$$\Delta\mathbf{\Gamma}_{n,r,c}(t+\Delta t) = \mathbf{\Gamma}_{n,r,c}(t+\Delta t) - \mathbf{\Gamma}_{n,r,c}(t) \quad (34)$$

Noted that the state of the previous time step  $\mathbf{A}_{n,r,c}(t)$ ,  $\mathbf{V}_{n,r,c}(t)$  and the incremental forcing vector of the new time step  $\Delta\mathbf{\Gamma}_{n,r,c}(t+\Delta t)$  are used to get the new displacement  $\mathbf{X}_{n,r,c}(t+\Delta t)$  via Eqs. (32) and (33). This is an implicit time iteration scheme. With any known initial conditions  $\mathbf{X}_{n,r,c}(0)$ ,  $\mathbf{V}_{n,r,c}(0)$ ,  $\mathbf{A}_{n,r,c}(0)$  and known time-varying force, EOMs Eq. (12) can be solved with this scheme.

Substitution of the  $\mathbf{X}_{n,r,c}(t)$ , i.e.,  $a_{n,r,c}(t)$ ,  $b_{n,r,c}(t)$ ,  $c_{n,r,c}(t)$  solved from Eq. (33) and the solutions for Eq. (24) into Eq. (21), then with combination of solutions for the other components which can be solved for similarly, leads to the time-variant displacements of the ring's centroid, as given by Eq. (19). Consequently, the time-variant displacements of any point on the ring can be obtained via Eq. (1). The accelerations and velocities are obtained analogously using the time derivatives of  $a_{n,r,c}(t)$ ,  $b_{n,r,c}(t)$  and  $c_{n,r,c}(t)$ .

In order to get the time domain solution for the unilateral foundation case, it is assumed that the status for previous time step at time  $t$ ,  $\hat{\mathbf{X}}(t)$ ,  $\hat{\mathbf{V}}(t)$  and  $\hat{\mathbf{A}}(t)$  are already known. If the increments from time  $t$  to  $t+\Delta t$  for the unilateral foundation can be solved for, the solution for any time point can be obtained via a time iterative scheme. We still use cosine component in the radial direction of  $n^{\text{th}}$  harmonic to illustrate the procedure. Considering the transition from time  $t$  to  $t+\Delta t$ , based on the linear foundation model, the displacement increment given by Eq. (32) can be written in terms of the state of the previous time step, and the mass, damping and linear stiffness matrices:

$$\begin{aligned} \Delta\hat{\mathbf{X}}_{n,r,c}(t+\Delta t) &= \frac{1}{2} \frac{\Delta t (\mathbf{C}_{n,r,c}\alpha\Delta t^2 + 2\mathbf{C}_{n,r,c}\beta\Delta t^2 - \mathbf{C}_{n,r,c}\Delta t^2 - \mathbf{M}_{n,r,c}\Delta t)}{-\mathbf{K}_{n,r,c}\beta\Delta t^2 + \mathbf{C}_{n,r,c}\alpha\Delta t - \mathbf{C}_{n,r,c}\Delta t - \mathbf{M}_{n,r,c}} \hat{\mathbf{A}}_{n,r,c}(t) \\ &+ \frac{1}{2} \frac{\Delta t (2\mathbf{C}_{n,r,c}\alpha\Delta t - 2\mathbf{C}_{n,r,c}\Delta t - 2\mathbf{M}_{n,r,c})}{-\mathbf{K}_{n,r,c}\beta\Delta t^2 + \mathbf{C}_{n,r,c}\alpha\Delta t - \mathbf{C}_{n,r,c}\Delta t - \mathbf{M}_{n,r,c}} \hat{\mathbf{V}}_{n,r,c}(t) \\ &- \frac{\Delta t^2\beta}{-\mathbf{K}_{n,r,c}\beta\Delta t^2 + \mathbf{C}_{n,r,c}\alpha\Delta t - \mathbf{C}_{n,r,c}\Delta t - \mathbf{M}_{n,r,c}} \Delta\mathbf{\Gamma}_{n,r,c}(t+\Delta t) \end{aligned} \quad (35)$$

Then, the new displacement of the current time step is:

$$\hat{\mathbf{X}}_{n,r,c}(t+\Delta t) = \hat{\mathbf{X}}_{n,r,c}(t) + \Delta\hat{\mathbf{X}}_{n,r,c}(t+\Delta t) \quad (36)$$

Correspondingly,  $\hat{u}_r(R, \theta, t + \Delta t)$  and  $\Delta \hat{u}_r(R, \theta, t + \Delta t)$  are obtained, although the linear stiffness matrix  $\mathbf{K}_{n,r,c}$  is utilized. Compared with the collapsible foundation, where foundation force vanishes in the region where  $\hat{u}_r(R, \theta, t + \Delta t) < 0$ , the transition from time  $t$  to  $t + \Delta t$  computed via Eqs. (35) and (36) includes effects by an excessive force in that region. The magnitude of this excessive force at time  $t + \Delta t$  is proportional to the displacement increment  $\Delta \hat{u}_r(R, \theta, t + \Delta t)$ , but the region is determined by the total displacement  $\hat{u}_r(R, \theta, t + \Delta t)$ . That is,

$$F_e^{t+\Delta t}(\theta) = \begin{cases} \Delta \hat{u}_r(R, \theta, t + \Delta t) K_r, & \{\theta | \theta \in \hat{u}_r(R, \theta, t + \Delta t) < 0\} \\ 0, & \{\theta | \theta \in \hat{u}_r(R, \theta, t + \Delta t) \geq 0\} \end{cases} \quad (37)$$

For a tensionless foundation case, this excessive force exists in the opposite region where  $\hat{u}_r(R, \theta, t + \Delta t) > 0$ , but all the remaining analysis will be the same.

Similar to the static case we outlined in [3], a compensation force can be applied to the linear foundation model to counter-act the excessive force at the current time step:

$$F_{cp}^{t+\Delta t}(\theta) = F_e^{t+\Delta t}(\theta) \quad (38)$$

Applying Fourier expansion to Eq. (38) within  $[-\pi, \pi]$ , and using the same mode numbers as  $\vec{F}(\theta)$ :

$$F_{cp}^{t+\Delta t}(\theta) = \sum_{n=-N}^N F_{cp,n}^{t+\Delta t}(\theta) = \sum_{n=-N}^N \left[ H_{n,r,c}^{t+\Delta t} \cos(n\theta) + H_{n,r,s}^{t+\Delta t} \sin(n\theta) \right] \quad (39)$$

where  $F_{cp,n}^{t+\Delta t}$  is the compensation force of  $n^{th}$  harmonic for the current time step;  $H_{n,r,c}^{t+\Delta t}$  and  $H_{n,r,s}^{t+\Delta t}$  are the Fourier coefficients. Because the unilateral property of the foundation only exists in the radial direction, this compensation force only has radial components. Again, we only take the cosine part in the following derivation, merely for simplicity and clarity.

The compensation force from Eq. (39) needs to be applied to the linear foundation model at the current time step to obtain the displacements for the unilateral foundation case. Using the analogy between  $p_{r,c}(t)Q_{n,r,c}$  in Eq. (17) (which is incorporated into  $\Gamma_{n,r,c}$  of Eq. (25)) and  $H_{n,r,c}^{t+\Delta t}$  in Eq. (39), the forcing vector due to the  $n^{th}$  harmonic compensation force for the current time step can be given by:

$$\Gamma_{cp,n,r,c}^{t+\Delta t} = \left[ \frac{H_{n,r,c}^{t+\Delta t}}{p_{r,c}(t+\Delta t)Q_{n,r,c}} \right] \Gamma_{n,r,c}(t+\Delta t) = \left[ \frac{H_{n,r,c}^{t+\Delta t}}{Q_{n,r,c}} \right] \Gamma_{n,r,c}^s \quad (40)$$

Now, the forcing vector applied to the linear foundation model at the current time step are:

$$\Gamma_{n,r,c}(t+\Delta t) + \Gamma_{cp,n,r,c}^{t+\Delta t} = \left[ p_{r,c}(t+\Delta t) + \frac{H_{n,r,c}^{t+\Delta t}}{Q_{n,r,c}} \right] \Gamma_{n,r,c}^s \quad (41)$$

The forcing vector increment at the current time step is then obtained via analogy to Eq. (41):

$$\Delta \Gamma_{n,r,c}(t+\Delta t) + \Gamma_{cp,n,r,c}^{t+\Delta t} = \left[ \Delta p_{r,c}(t+\Delta t) + \frac{H_{n,r,c}^{t+\Delta t}}{Q_{n,r,c}} \right] \Gamma_{n,r,c}^s \quad (42)$$

Then, the compensated displacement increment is obtained by replacing the external forcing vector increment  $\Delta \Gamma_{n,r,c}(t+\Delta t)$  in Eq. (35) with the compensated one in Eq. (42):

$$\begin{aligned} \Delta \hat{\mathbf{X}}_{n,r,c}(t+\Delta t) &= \frac{1}{2} \frac{\Delta t (\mathbf{C}_{n,r,c} \alpha \Delta t^2 + 2\mathbf{C}_{n,r,c} \beta \Delta t^2 - \mathbf{C}_{n,r,c} \Delta t^2 - \mathbf{M}_{n,r,c} \Delta t) \hat{\mathbf{A}}_{n,r,c}(t)}{-\mathbf{K}_{n,r,c} \beta \Delta t^2 + \mathbf{C}_{n,r,c} \alpha \Delta t - \mathbf{C}_{n,r,c} \Delta t - \mathbf{M}_{n,r,c}} \\ &+ \frac{1}{2} \frac{\Delta t (2\mathbf{C}_{n,r,c} \alpha \Delta t - 2\mathbf{C}_{n,r,c} \Delta t - 2\mathbf{M}_{n,r,c}) \hat{\mathbf{V}}_{n,r,c}(t)}{-\mathbf{K}_{n,r,c} \beta \Delta t^2 + \mathbf{C}_{n,r,c} \alpha \Delta t - \mathbf{C}_{n,r,c} \Delta t - \mathbf{M}_{n,r,c}} \\ &- \frac{\Delta t^2 \beta}{-\mathbf{K}_{n,r,c} \beta \Delta t^2 + \mathbf{C}_{n,r,c} \alpha \Delta t - \mathbf{C}_{n,r,c} \Delta t - \mathbf{M}_{n,r,c}} \left[ \Delta p_{r,c}(t+\Delta t) + \frac{H_{n,r,c}^{t+\Delta t}}{Q_{n,r,c}} \right] \Gamma_{n,r,c}^s \end{aligned} \quad (43)$$

The new increment in Eq. (43) and the corresponding new displacement via Eq. (36) lead to new references to obtain the excessive force in Eq. (37). This leads to an iterative scheme within each time step which is deemed to converge when the re-computation of Eq. (36) to Eq. (43) only leads to a change that is smaller than a threshold. Once converged,  $\hat{\mathbf{X}}_{n,r,c}(t+\Delta t)$  is plugged into Eq. (31) to get new  $\hat{\mathbf{A}}_{n,r,c}(t+\Delta t)$  and  $\hat{\mathbf{V}}_{n,r,c}(t+\Delta t)$  for the iteration to the next time step.

The three remaining components in Eq. (19) for the unilateral foundation can be solved for by following the same procedure, so that the final solution for the unilateral case is obtained via the Eq. (19).

It is worth mentioning due to the fact that the constant linear stiffness matrix is used, all the matrices ( $\mathbf{K}_{n,r,c}$ ,  $\mathbf{C}_{n,r,c}$ ,  $\mathbf{M}_{n,r,c}$ ) used in Eq. (43) are constant and time-invariant. This means that they can be pre-computed and inverted only once at the beginning of the whole time-series computation. The compensated forcing vector increment Eq. (42) can be obtained algebraically from the one before compensation that appears in the 3rd term on right hand side of Eq. (35), via the proportional relationships of  $Q_{n,r,c}$  and  $H_{n,r,c}$ . This helps to avoid time consuming matrix inversions in the computation of displacements Eq. (43) at every time step. This is a clear advantage compared with conventional nonlinear implicit time integration methods which rely on matrix inversions during the nonlinear iterations of each time step.

### 3.3. Axle force transmission

The force transmitted to the axle is an important factor that affects ride comfort in tire applications. In the REF model, the foundation is essentially modeled as continuous spring with viscous damping in the radial and circumferential directions via  $K_r$ ,  $K_\theta$  and viscous damping  $C_{Er}$ ,  $C_{E\theta}$ . The force transmitted to the axle/ring center by the foundation is therefore readily related to the velocity and deformation of the foundation. The radial and circumferential displacements of the foundation, which are the same as the radial and circumferential displacement of the internal rim of the ring, are given via Eq. (1):

$$\begin{aligned} u_{r,f}(\theta, t) &= u_r\left(R - \frac{h}{2}, \theta, t\right) = u_r(R, \theta, t) \\ u_{\theta,f}(\theta, t) &= u_\theta\left(R - \frac{h}{2}, \theta, t\right) = u_\theta(R, \theta, t) - \frac{h}{2}\phi(R, \theta, t) \end{aligned} \tag{44}$$

Consequently, the velocities of the foundation in both the radial and circumferential direction are given by:

$$\begin{aligned} \frac{\partial}{\partial t} u_{r,f}(\theta, t) &= \frac{\partial}{\partial t} u_r(R, \theta, t) \\ \frac{\partial}{\partial t} u_{\theta,f}(\theta, t) &= \frac{\partial}{\partial t} u_\theta(R, \theta, t) - \frac{h}{2} \frac{\partial}{\partial t} \phi(R, \theta, t) \end{aligned} \tag{45}$$

The force components induced by radial stiffness and damping needs to exclude the vanished region due to the unilateral property of the foundation:

$$\begin{aligned} F_{Az,r}(t) &= \int_{-\pi}^{\pi} - [u_{r,f}(\theta, t)K_r + \frac{\partial}{\partial t} u_{r,f}(\theta, t)C_{Er}] \cos(\theta) d\theta & \begin{cases} \theta | \theta \in u_{r,f}(\theta, t) > 0 & \text{Collapsible Foundation} \\ \theta | \theta \in u_{r,f}(\theta, t) < 0 & \text{Tensionless Foundation} \end{cases} \\ F_{Ax,r}(t) &= \int_{-\pi}^{\pi} [u_{r,f}(\theta, t)K_r + \frac{\partial}{\partial t} u_{r,f}(\theta, t)C_{Er}] \sin(\theta) d\theta \end{aligned} \tag{46}$$

where  $F_{Az,r}$  is vertical axle force induced by radial stiffness and damping, while  $F_{Ax,r}$  represents the corresponding horizontal axle force.

The force components induced by the circumferential stiffness and damping is the integration over the whole ring circumference since no vanished region considered:

$$\begin{aligned} F_{Az,t}(t) &= \int_{-\pi}^{\pi} \left[ u_{\theta,f}(\theta, t)K_r + \frac{\partial}{\partial t} u_{\theta,f}(\theta, t)C_{Er} \right] \sin(\theta) d\theta \\ F_{Ax,t}(t) &= \int_{-\pi}^{\pi} \left[ u_{\theta,f}(\theta, t)K_r + \frac{\partial}{\partial t} u_{\theta,f}(\theta, t)C_{Er} \right] \cos(\theta) d\theta \end{aligned} \tag{47}$$

Then the total axle forces are the summations of the two components, respectively:

$$\begin{aligned} F_{Az}(t) &= F_{Az,r}(t) + F_{Az,t}(t) \\ F_{Ax}(t) &= F_{Ax,r}(t) + F_{Ax,t}(t) \end{aligned} \tag{48}$$

## 4. Illustrative examples

In this section, two examples are given to show the application of the approach presented above. First, the results for the pulse force response are shown and compared with Finite Element Analysis (FEA) results; then chirp force response is shown and used to analyze the frequency response and axle force transmissibility. A radial concentrated force, which only contains radial and cosine component in its Fourier expansion, is applied at the circumferential coordinate ( $\theta = 0$ ) (called loaded point, hereafter). Due to the similarity and analogy between the radial or circumferential and cosine or sine component permutations in the form of Fourier series, solutions for any more complex circumferentially distributed force follow similarly as discussed in Section 3.

### 4.1. Pulse response and comparison with FEA results

The time-varying radial concentrated force can be represented in the form of a function with respect to  $\theta$  and  $t$ :

$$f_c(\theta, t) = p(t) \frac{1}{2\pi} Q \sum_{n=-N}^N e^{-\frac{1}{4} n^2 \sigma^2} \cos(n\theta) \tag{49}$$

where time-varying function  $p(t)$  controls the signal shape in the time domain.  $\sigma$  is a parameter that determines how concentrated the force is in the distribution with respect to  $\theta$ .  $Q$  is the magnitude of the concentrated force. In this case  $Q = -1000\text{N}$  is used, where the minus sign indicates the force is pointing to the ring's center. From Eqs. (49) and (17), Fourier coefficient  $Q_{n,r,c}$  can be obtained by:

$$Q_{n,r,c} = \frac{1}{2\pi} Q e^{-\frac{1}{4} n^2 \sigma^2} \tag{50}$$

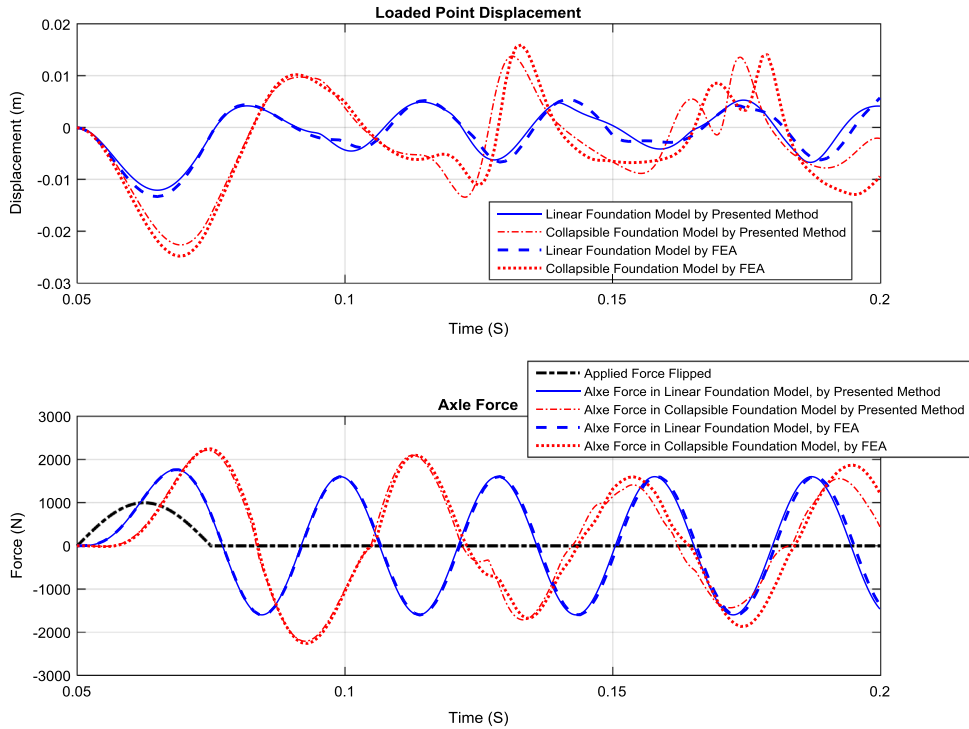


Fig. 2. Pulse response and comparison with FEA results.

A collapsible unilateral foundation is considered. The values of the model parameters are listed in Table 1, where geometry and material parameters are mainly adopted from [2] with minor changes. But parameters specifically for dynamic performance are added and selected for illustration purposes.

An equivalent 2D Finite Element model is established using Abaqus software to compare with the presented solution method. The thick ring is meshed using the Timoshenko beam element B21, with 360 divisions circumferentially. The radial stiffness of the foundation is modeled via a set of 360 evenly distributed and independent linear or nonlinear *Spring2* elements, and the circumferential stiffness is generated by another set of 360 linear *Spring2* elements. The stiffness of every linear spring element, or the effective non-vanished stiffness for the nonlinear spring element representing the unilateral foundation, is obtained by:

$$\begin{aligned}
 k_r &= \frac{2 \pi K_r}{N_r} \\
 k_\theta &= \frac{2 \pi K_\theta}{N_\theta}
 \end{aligned}
 \tag{51}$$

where  $N_r = N_\theta = 360$  are number of spring elements in the radial and circumferential directions, respectively. The dynamic response is obtained using Abaqus/Standard solver.

Since the way that Abaqus software models damping is different from the one used in the above EOMs, the comparative simulations are done by excluding damping (setting to zero) in both models.

The time responses of the loaded point (bottom point) displacement as well as the axle force are shown in Fig. 2 and compared with FEA results. It can be seen that the results match rather closely, especially for the axle force response in linear foundation case. Remaining deviations can be explained by the substantial differences in the two approaches. The FEA model is a discretized model, where the REF model is approximated by a polygon with 360 edges and 360 sets of discretized spring elements. The Timoshenko beam elements are assigned to equivalent geometry and stiffness parameters, but the thickness effect is only approximately accounted for by internal functions of these elements. In our parametric REF model and analytical solution method, different approximations exist, such as section inertia approximations made in Eq. (15), finite mode numbers ( $N = 50$ ), etc. From this perspective, the existing small deviations in the results can be reasonable and acceptable.

It can also be seen that the deviations in the results obtained by the two approaches are larger for the case of nonlinear (unilateral) foundation. In particular, the deviations increase with time. These increasing deviations with time are caused by accumulations of errors and are typical for time integrations of nonlinear systems [23]. It can be proved that integration errors are bounded for linear systems but not guaranteed for nonlinear systems [24]. The early time duration which shows reduced deviation (Fig. 2) can be extended by using smaller time steps [24], but this cannot be extended to infinity due to the substantial properties of nonlinear systems. This is a fundamental limitation of our proposed method in solving

unilateral foundation problems. However, due to the so-called butterfly effect in the nonlinear systems [23], it can be inferred that even the real tests (or more detailed FEA models), small and random disturbances will give different responses in different transient test results. Furthermore, in practice, the magnitude of the first peak (with small time interval) is more important since in the real system, the following peaks will be damped out gradually. For this standpoint, the predictions of the model could be acceptable.

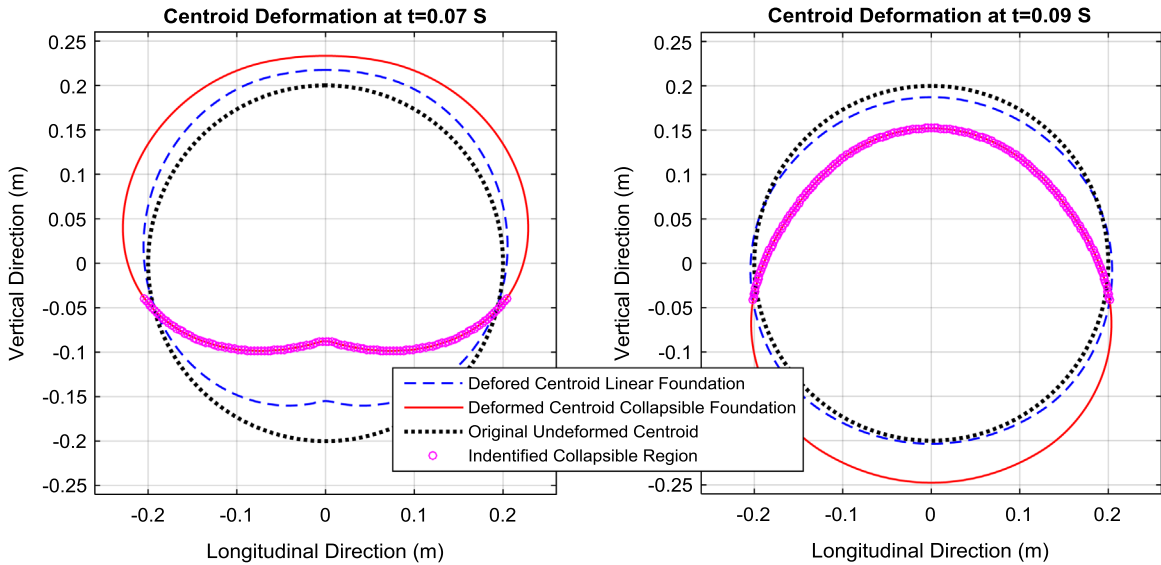


Fig. 3. Deformation of ring centroid at different time points.

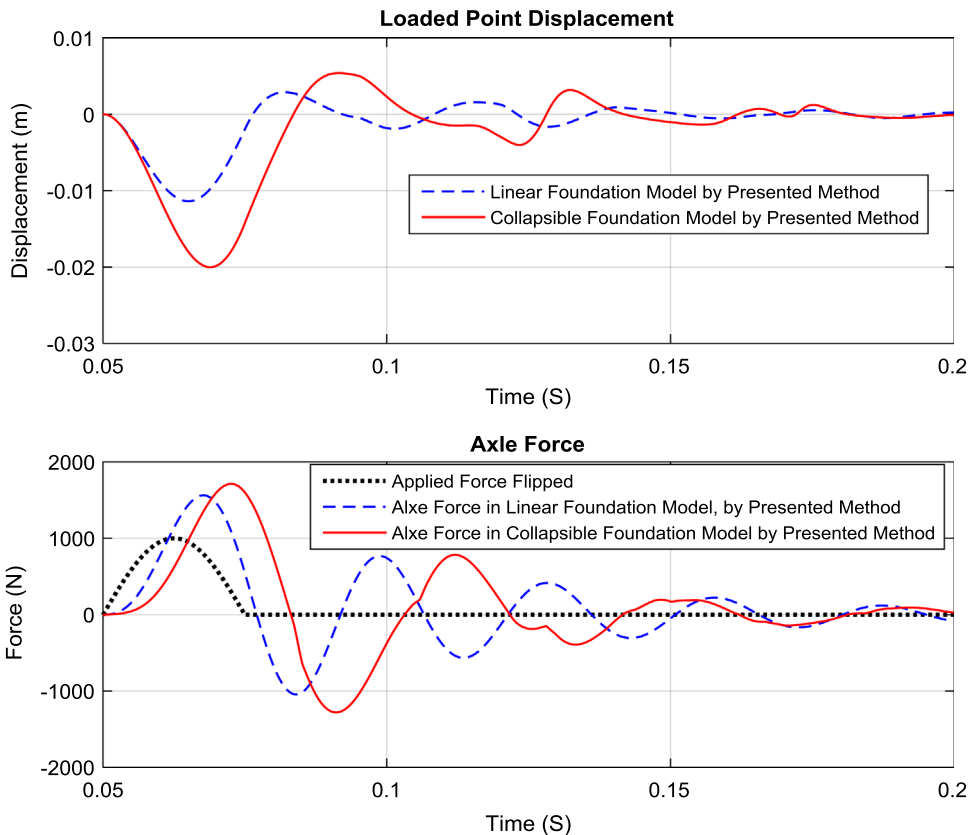


Fig. 4. Loaded point displacement and axle force.

Fig. 3 shows the deformations of the ring’s centroid at select time points, with the magnitudes of displacements amplified by 5 times. At around  $t = 0.07s$ , the compression of the loaded point in the unilateral foundation case approaches its maximum magnitude, and bounces back at around  $t = 0.09s$ . For every time point, the identified collapsible regions of the foundation are also shown in small magenta circles on top of the deformed centroid of collapsible foundation case.

Fig. 4 shows the responses for the damped systems, where viscous damping density in radial and circumferential directions of the foundation are given by:

$$C_{Er} = C_{E\theta} = 50N \text{ s radian}^{-1}m^{-1} \tag{52}$$

It can be found from both Figs. 2 and 4 that with the same exciting force, the magnitudes of responses are higher in the unilateral foundation model than those in the linear foundation model. Meanwhile, the response frequencies are lower due to partially missing foundation stiffness.

#### 4.2. Chirp signal response

The frequency response and axle force transmissibility of the unilateral foundation problem can be studied via the chirp signal response. In this example, a chirp signal with frequency range from 10 Hz to 100 Hz is used. The peak to peak magnitude of the chirp signal is set to 40N. The chirp signal is offset by a static force with magnitude  $\pm 1000N$ . These opposite offsets lead to chirp forces in different directions. The time response to these opposite chirp forces by both the unilateral and linear foundations are analyzed in the frequency domain and the results are shown in Fig. 5. The left column shows the results for collapsible foundation and the right column is for linear foundation. The frequency content for the applied chirp force is shown in the bottom row. It can be seen that the dominant components are between 20 Hz and 90 Hz and float around a mean value. And the static offset (positive or negative 1000 N) of the chirp force do not affect the magnitude of the frequency components at all. The top and the middle rows show the frequency analysis results for the displacement of the loaded point and for the axle force, respectively. For the unilateral foundation, it can be seen that the resonance frequencies of the loaded point oscillation and axle force are different for the chirp force offset by a positive or

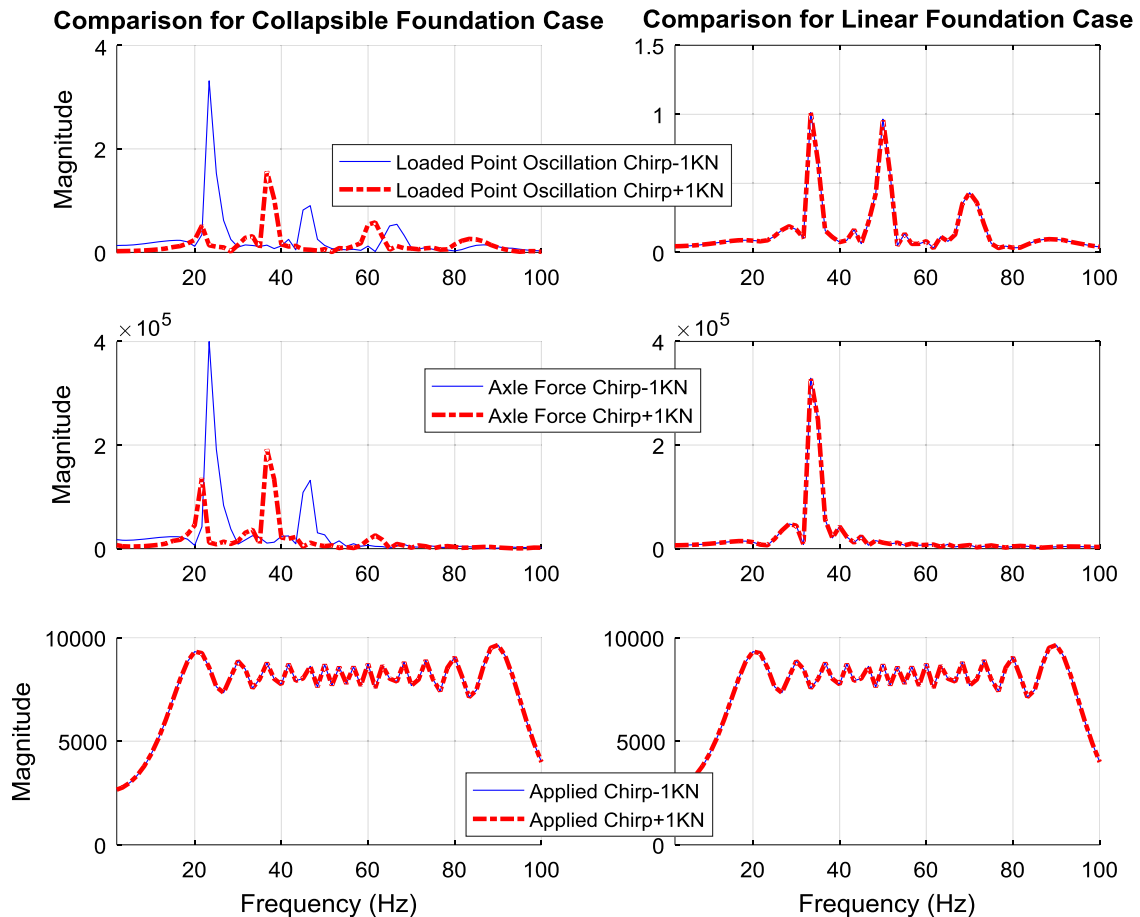


Fig. 5. Comparison of frequency response to chirp signal with different offset.

negative magnitude. However, for the linear foundation case, they are the same for either positive or negative offset. The different resonance frequencies for the unilateral foundation case are a manifestation of the different stiffnesses when the ring on unilateral foundation is compressed or stretched.

## 5. Conclusions and future work

This paper considered the in-plane dynamics of a ring on a unilateral elastic foundation model, which is suitable for the parametric studies in the design space exploration of non-pneumatic tires, or bushing bearings. It dealt with a two-parameter elastic foundation that is linear circumferentially, but unilateral in the radial direction where the radial stiffness of the foundation vanishes when compressed or tensioned. The difficulty of this nonlinear problem lies in the fact that the stiffness of the foundation changes with the deformation state of the ring and vice versa. A general orthotropic and extensible thick ring is considered and modeled via Timoshenko beam theory. An approach that combines a new iterative spatial compensation scheme integrated with a Newmark implicit time integration method is presented to solve the in-plane vibration problem.

Compared with discretization-based numerical methods such as nonlinear FEA, the advantages of the proposed iterative approach are three-fold: 1) Time-consuming modeling and meshing work is avoided. This is specially attractive in the parametric studies at the design stage for the application (e.g. non-pneumatic tires and bushing bearings). 2) Only matrices of dimensions of  $3 \times 3$  are involved in computations at every time step, corresponding to the 3 variables of the Timoshenko beam; while the dimensions of the matrices in the FEA depend on the number of the nodes, which is generally a lot higher than 3 to sufficiently describe a thick ring. 3) The iterations at every time step are based on the linear foundation model, where system matrices, specially the stiffness matrix, is constant and time invariant. So the matrix only needs to be inverted once at the beginning of the whole computation. However, in the nonlinear implicit FEA methods, the nonlinear stiffness matrix is time variant and the time consuming matrix inversion needs to be implemented at every nonlinear iteration of each time step.

In our future work, this approach will be extended to solve even more complex dynamics problems involving a ring on unilateral foundation. This includes the dynamic contact problem where the computation efficiency of the approach can be exploited to solve for the response of the system involving contact with arbitrary geometry surfaces.

## Appendix A. Coefficients of EOMs

$$\begin{aligned}
 Ca_{2,1} &= \rho hR \cdot u_{r,n,r,c}(R, \theta) \\
 Ca_{1,1} &= \frac{C_{er}}{b} \cdot u_{r,n,r,c}(R, \theta) \\
 Ca_{0,1} &= -\frac{GA}{bR} \cdot \frac{\partial^2}{\partial \theta^2} u_{r,n,r,c}(R, \theta) + \left( \frac{K_r}{b} - \frac{EA_\theta}{(\nu_{\theta r} \nu_{r\theta} - 1)Rb} \right) \cdot u_{r,n,r,c}(R, \theta) \\
 Cb_{0,1} &= \left( \frac{GA}{bR} - \frac{EA_\theta}{(\nu_{\theta r} \nu_{r\theta} - 1)Rb} \right) \cdot \frac{\partial}{\partial \theta} u_{\theta,n,r,c}(R, \theta) \\
 Cc_{0,1} &= -\frac{GA}{b} \cdot \frac{\partial}{\partial \theta} \phi_{n,r,c}(R, \theta)
 \end{aligned} \tag{A.1}$$

$$\begin{aligned}
 Ca_{0,2} &= \left( \frac{EA_\theta}{(\nu_{\theta r} \nu_{r\theta} - 1)Rb} - \frac{GA}{bR} \right) \cdot \frac{\partial}{\partial \theta} u_{r,n,r,c}(R, \theta) \\
 Cb_{2,2} &= \rho hR \cdot u_{\theta,n,r,c}(R, \theta) \\
 Cb_{1,2} &= \frac{C_{e\theta}}{b} \cdot u_{\theta,n,r,c}(R, \theta) \\
 Cb_{0,2} &= \frac{EA_\theta}{(\nu_{\theta r} \nu_{r\theta} - 1)Rb} \cdot \frac{\partial^2}{\partial \theta^2} u_{\theta,n,r,c}(R, \theta) + \left( \frac{GA}{bR} + \frac{K_\theta}{b} \right) \cdot u_{\theta,n,r,c}(R, \theta) \\
 Cc_{2,2} &= \frac{1}{12} \rho h^3 \cdot \phi_{n,r,c}(R, \theta) \\
 Cc_{1,2} &= -\frac{1}{2} \frac{C_{e\theta} h}{b} \cdot \phi_{n,r,c}(R, \theta) \\
 Cc_{0,2} &= -\left( \frac{GA}{b} + \frac{K_\theta h}{2b} \right) \cdot \phi_{n,r,c}(R, \theta)
 \end{aligned} \tag{A.2}$$

$$\begin{aligned}
 Ca_{0,3} &= \frac{GA}{b} \cdot \frac{\partial}{\partial \theta} u_{r,n,r,c}(R, \theta) \\
 Cb_{2,3} &= \frac{1}{12} \rho h^3 \cdot u_{\theta,n,r,c}(R, \theta)
 \end{aligned}$$

$$\begin{aligned}
 Cb_{1,3} &= -\frac{1}{2} \frac{C_{e\theta} h}{b} \cdot u_{\theta,n,r,c}(R, \theta) \\
 Cb_{0,3} &= -\left(\frac{GA}{b} + \frac{K_{\theta} h}{2b}\right) \cdot u_{\theta,n,r,c}(R, \theta) \\
 Cc_{2,3} &= \frac{1}{12} \rho h^3 R \cdot \phi_{n,r,c}(R, \theta) \\
 Cc_{1,3} &= \frac{1}{4} \frac{C_{e\theta} h^2}{b} \cdot \phi_{n,r,c}(R, \theta) \\
 Cc_{0,3} &= \left(\frac{GA \cdot R}{b} + \frac{h^2 K_{\theta}}{4b}\right) \cdot \phi_{n,r,c}(R, \theta) + \frac{EI_{\theta}}{(\nu_{\theta r} \nu_{r\theta} - 1)Rb} \cdot \frac{\partial^2}{\partial \theta^2} \phi_{n,r,c}(R, \theta)
 \end{aligned} \tag{A.3}$$

$$\begin{aligned}
 Cp_1 &= \frac{1}{b} Q_{n,r,c} \cos(n\theta) \\
 Cp_2 &= 0 \\
 Cp_3 &= 0
 \end{aligned} \tag{A.4}$$

**Appendix B. Solutions for static system**

$$\begin{aligned}
 u_{r,n,r,c}(R, \theta) &= \frac{Zurn4\_rc \cdot n^4 + Zurn2\_rc \cdot n^2 + Zurn0\_rc}{ZDn6\_rc \cdot n^6 + ZDn4\_rc \cdot n^4 + ZDn2\_rc \cdot n^2 + ZDn0\_rc} Q_{nrc} \cos(n\theta) \\
 u_{\theta,n,r,c}(R, \theta) &= \frac{Zutn3\_rc \cdot n^3 + Zutn1\_rc \cdot n}{ZDn6\_rc \cdot n^6 + ZDn4\_rc \cdot n^4 + ZDn2\_rc \cdot n^2 + ZDn0\_rc} Q_{nrc} \sin(n\theta) \\
 \phi_{n,r,c}(R, \theta) &= \frac{Zphin3\_rc \cdot n^3 + Zphin1\_rc \cdot n}{ZDn6\_rc \cdot n^6 + ZDn4\_rc \cdot n^4 + ZDn2\_rc \cdot n^2 + ZDn0\_rc} Q_{nrc} \sin(n\theta)
 \end{aligned} \tag{B.1}$$

$$\begin{aligned}
 ZDn6\_rc &= 4 GA EA_{\theta} EI_{\theta} \\
 ZDn4\_rc &= (-GA h^2 \nu_{\theta r} \nu_{r\theta} EA_{\theta} K_{\theta} + GA h^2 EA_{\theta} K_{\theta} - 4 GA \nu_{\theta r} \nu_{r\theta} EI_{\theta} K_{\theta} + 4 GA EI_{\theta} K_{\theta} + 4 K_r EA_{\theta} EI_{\theta})R \\
 &\quad - 8 GA EA_{\theta} EI_{\theta} \\
 ZDn2\_rc &= (-4 GA K_r \nu_{\theta r} \nu_{r\theta} EA_{\theta} + 4 GA K_r EA_{\theta})R^3 \\
 &+ (-K_r h^2 \nu_{\theta r} \nu_{r\theta} EA_{\theta} K_{\theta} - 4 GA h \nu_{\theta r} \nu_{r\theta} EA_{\theta} K_{\theta} + K_r h^2 EA_{\theta} K_{\theta} - 4 K_r \nu_{\theta r} \nu_{r\theta} EI_{\theta} K_{\theta} + 4 GA h EA_{\theta} K_{\theta} + 4 K_r EI_{\theta} K_{\theta})R^2 \\
 &+ (2 GA h^2 \nu_{\theta r} \nu_{r\theta} EA_{\theta} K_{\theta} - 4 GA K_r \nu_{\theta r} \nu_{r\theta} EI_{\theta} - 2 GA h^2 EA_{\theta} K_{\theta} + 4 GA K_r EI_{\theta} + 4 EA_{\theta} EI_{\theta} K_{\theta})R + 4 GA EA_{\theta} EI_{\theta} \\
 ZDn0\_rc &= (4 GA K_r \nu_{\theta r}^2 \nu_{r\theta}^2 K_{\theta} - 8 GA K_r \nu_{\theta r} \nu_{r\theta} K_{\theta} + 4 GA K_r K_{\theta})R^4 \\
 &+ (-4 GA K_r h \nu_{\theta r}^2 \nu_{r\theta}^2 K_{\theta} + 8 GA K_r h \nu_{\theta r} \nu_{r\theta} K_{\theta} - 4 GA \nu_{\theta r} \nu_{r\theta} EA_{\theta} K_{\theta} - 4 GA K_r h K_{\theta} + 4 GA EA_{\theta} K_{\theta})R^3 \\
 &+ (GA K_r h^2 \nu_{\theta r}^2 \nu_{r\theta}^2 K_{\theta} - 2 GA K_r h^2 \nu_{\theta r} \nu_{r\theta} K_{\theta} + 4 GA h \nu_{\theta r} \nu_{r\theta} EA_{\theta} K_{\theta} + GA K_r h^2 K_{\theta} - 4 GA h EA_{\theta} K_{\theta})R^2 \\
 &+ (-GA h^2 \nu_{\theta r} \nu_{r\theta} EA_{\theta} K_{\theta} + GA h^2 EA_{\theta} K_{\theta})R
 \end{aligned} \tag{B.2}$$

$$\begin{aligned}
 Zurn4\_rc &= 4 REA_{\theta} EI_{\theta} \\
 Zurn2\_rc &= (-4 GA \nu_{\theta r} \nu_{r\theta} EA_{\theta} + 4 GA EA_{\theta})R^3 \\
 &+ (-h^2 \nu_{\theta r} \nu_{r\theta} EA_{\theta} K_{\theta} + h^2 EA_{\theta} K_{\theta} - 4 \nu_{\theta r} \nu_{r\theta} EI_{\theta} K_{\theta} + 4 EI_{\theta} K_{\theta})R^2 \\
 &\quad + (-4 GA \nu_{\theta r} \nu_{r\theta} EI_{\theta} + 4 GA EI_{\theta})R \\
 Zurn0\_rc &= (4 GA \nu_{\theta r}^2 \nu_{r\theta}^2 K_{\theta} - 8 GA \nu_{\theta r} \nu_{r\theta} K_{\theta} + 4 GA K_{\theta})R^4 \\
 &+ (-4 GA h \nu_{\theta r}^2 \nu_{r\theta}^2 K_{\theta} + 8 GA h \nu_{\theta r} \nu_{r\theta} K_{\theta} - 4 GA h K_{\theta})R^3 \\
 &+ (GA h^2 \nu_{\theta r}^2 \nu_{r\theta}^2 K_{\theta} - 2 GA h^2 \nu_{\theta r} \nu_{r\theta} K_{\theta} + GA h^2 K_{\theta})R^2
 \end{aligned} \tag{B.3}$$

$$\begin{aligned}
 Zutn3\_rc &= 4 EI_{\theta} (GA \nu_{\theta r} \nu_{r\theta} - GA - EA_{\theta})R \\
 Zutn1\_rc &= (2 GA h \nu_{\theta r}^2 \nu_{r\theta}^2 K_{\theta} - 4 GA h \nu_{\theta r} \nu_{r\theta} K_{\theta} + 4 GA \nu_{\theta r} \nu_{r\theta} EA_{\theta} + 2 GA h K_{\theta} - 4 GA EA_{\theta})R^3 \\
 &+ (-GA h^2 \nu_{\theta r}^2 \nu_{r\theta}^2 K_{\theta} + 2 GA h^2 \nu_{\theta r} \nu_{r\theta} K_{\theta} + h^2 \nu_{\theta r} \nu_{r\theta} EA_{\theta} K_{\theta} - GA h^2 K_{\theta} - h^2 EA_{\theta} K_{\theta})R^2
 \end{aligned} \tag{B.4}$$

$$\begin{aligned}
Z_{\text{phin3\_rc}} &= -4 R^2 GA EA_{\theta} (\nu_{\text{or}} \nu_{\text{r}\theta} - 1) \\
&\quad Z_{\text{phin1\_rc}} \\
&= (4 GA \nu_{\text{or}}^2 \nu_{\text{r}\theta}^2 K_{\theta} - 8 GA \nu_{\text{or}} \nu_{\text{r}\theta} K_{\theta} + 4 GA K_{\theta}) R^3 \\
&+ (-2 GA h \nu_{\text{or}}^2 \nu_{\text{r}\theta}^2 K_{\theta} + 4 GA h \nu_{\text{or}} \nu_{\text{r}\theta} K_{\theta} + 2 h \nu_{\text{or}} \nu_{\text{r}\theta} EA_{\theta} K_{\theta} + 4 GA \nu_{\text{or}} \nu_{\text{r}\theta} EA_{\theta} - 2 GA h K_{\theta} - 2 h EA_{\theta} K_{\theta} - 4 GA EA_{\theta}) R^2 \quad (\text{B.5})
\end{aligned}$$

## References

- [1] T.B. Rhyne, S.M. Cron, Development of a non-pneumatic wheel, *Tire Science and Technology* 34 (2006) 150–169.
- [2] A. Gasmí, P.F. Joseph, T.B. Rhyne, S.M. Cron, Development of a two-dimensional model of a compliant non-pneumatic tire, *International Journal of Solids and Structures* 49 (2012) 1723–1740.
- [3] C. Wang, B. Ayalew, T. Rhyne, S. Cron, B. Dailliez, Static analysis of a thick ring on a unilateral elastic foundation, *International Journal of Mechanical Sciences* 101–102 (2015) 429–436.
- [4] J.L. Lin, W. Soedel, On general in-plane vibrations of rotating thick and thin rings, *Journal of Sound and Vibration* 122 (1988) 547–570.
- [5] S.C. Huang, W. Soedel, Effects of Coriolis acceleration on the free and forced in-plane vibrations of rotating rings on elastic foundation, *Journal of Sound and Vibration* 115 (1987) 253–274.
- [6] Y.T. Wei, L. Nasdala, H. Rothert, Analysis of forced transient response for rotating tires using REF models, *Journal of Sound and Vibration* 320 (2009) 145–162.
- [7] S.C. Huang, B.S. Hsu, Approach to the dynamic analysis of rotating tire-wheel-suspension units, *Journal of Sound and Vibration* 156 (1992) 505–519.
- [8] S. Gong, A Study of In-plane Dynamics of Tires, Delft University of Technology, Faculty of Mechanical Engineering and Marine Technology 1993.
- [9] S. Noga, R. Bogacz, T. Markowski, Vibration analysis of a wheel composed of a ring and a wheel-plate modelled as a three-parameter elastic foundation, *Journal of Sound and Vibration* 333 (2014) 6706–6722.
- [10] X. Wu, R.G. Parker, Vibration of rings on a general elastic foundation, *Journal of Sound and Vibration* 295 (2006) 194–213.
- [11] G.R. Potts, C.A. Bell, L.T. Charek, T.K. Roy, Tire vibrations, *Tire Science and Technology* 5 (1977) 202–225.
- [12] M. Loo, A model analysis of tire behavior under vertical loading and straight-line free rolling, *Tire Science and Technology* 13 (1985) 67–90.
- [13] J.L. Lin, W. Soedel, Dynamic response of a rotating thick ring to force or displacement excitation, *Journal of Sound and Vibration* 121 (1988) 317–337.
- [14] J.L. Lin, W. Soedel, On the critical speeds of rotating thick or thin rings, *Mechanics of Structures and Machines* 16 (1988) 439–483.
- [15] D. Allaei, W. Soedel, T.Y. Yang, Eigenvalues of rings with radial spring attachments, *Journal of Sound and Vibration* 121 (1988) 547–561.
- [16] W. Rutherford, S. Bezzam, A. Proddaturi, L. Thompson, J.C. Ziegert, T.B. Rhyne, S.M. Cron, Use of orthogonal arrays for efficient evaluation of geometric designs for reducing vibration of a non-pneumatic wheel during high-speed rolling, *Tire Science and Technology* 38 (2010) 246–275.
- [17] Z. Celep, In-plane vibrations of circular rings on a tensionless foundation, *Journal of Sound and Vibration* 143 (1990) 461–471.
- [18] J. Kim, G.F. Dargush, Y.-K. Ju, Extended framework of Hamilton's principle for continuum dynamics, *International Journal of Solids and Structures* 50 (2013) 3418–3429.
- [19] A. Gasmí, P.F. Joseph, T.B. Rhyne, S.M. Cron, Closed-form solution of a shear deformable, extensional ring in contact between two rigid surfaces, *International Journal of Solids and Structures* 48 (2011) 843–853.
- [20] S.S. Rao, *Vibration of Continuous Systems*, Wiley, 2007.
- [21] J.W.S.B. Rayleigh, *The Theory of Sound*, Macmillan, 1894.
- [22] H. Zolghadr Jahromi, B.A. Izzuddin, Energy conserving algorithms for dynamic contact analysis using Newmark methods, *Computers and Structures* 118 (2013) 74–89.
- [23] J.M.T. Thompson, H.B. Stewart, *Nonlinear Dynamics and Chaos*, Wiley, 2002.
- [24] S.-Y. Chang, Studies of newmark method for solving nonlinear systems: (I) basic analysis, *Journal of the Chinese Institute of Engineers, Transactions of the Chinese Institute of Engineers, Series A/Chung-kuo Kung Ch'eng Hsueh K'an* 27 (2004) 651–662.